

Online Materials and Methods

Synthesis of ⁶⁴Cu-Macrin and ⁶⁴Cu-Macrin

Macrin is a spherically shaped dextran nanoparticle with a hydrodynamic diameter of ~20 nm¹⁵ which is composed of FDA-approved polyglucose, L-lysine cross-linkers and a radionuclide chelator. Macrin nanoparticles were synthesized from carboxymethylated polyglucose (4 kDa MW, 5% COOH, TdB consultancy) and L-lysine via amide bond formation. In brief, carboxyl groups were activated by the coupling reagents EDC and NHS, followed by cross linking through L-lysine in aqueous media. After ethanol precipitation and dialysis (MWCO 8-10 kDa), Macrin nanoparticles (NPs) were lyophilized and further functionalized. Amino groups of Macrin-NPs were conjugated with radioisotope chelators (NODA-GA-NHS, Chematek) or near infrared fluorophores (VT680-NHS, Perkin Elmer) for PET or optical imaging, respectively. Remaining amine residues were succinylated to prevent interactions with plasma proteins by increasing Macrin's negative surface charge. Unreacted small molecules were removed by size exclusion methods. Pure Macrin-NODA was lyophilized and stored at -20 °C until use. VT680Macrin was stored in phosphate buffered saline (PBS). Macrin-NODA was characterized by dynamic light scattering and zeta potential (Zetasizer Nano, Malvern Panalytical Instruments Inc.): hydrodynamic diameter 16.6 ± 1.6 nm, polydispersity index 0.29 ± 0.03 and zeta -6.46 ± 0.63 mV. ⁶⁴Cu-Macrin was prepared under metal-free conditions. Briefly, ⁶⁴CuCl₂ in 0.1 N HCl (University of Wisconsin) was added into Macrin-NODA buffer solution, and the mixture was incubated for 30 min at 90 °C. ⁶⁴Cu-Macrin (~20 MBq/μg Macrin) was obtained with ~95% radiochemical yield (decay-corrected) and >99% radiochemical purity, as determined by radio-TLC using a 50 mM aqueous EDTA solution as an eluent. Before administration to animals, Macrins were reconstituted with saline and sterilized using a 0.22 μm HT Tuffryn Membrane syringe filter (Pall Life Sci).

Mice

C57BL/6J (000664), Cx3cr1^{GFP/+} (B6.129P-Cx3cr1^{tm1Litt}/Jax strain #005582) and Apoe^{tm1Unc} (Apoe^{-/-}. 002052) mice were purchased from The Jackson Laboratory. Apoe^{-/-} mice were fed a Western diet (TD.88137, Envigo) starting at age of 10-wk for 14 weeks to develop atherosclerosis and analyzed 24 hrs after Macrin injection. C57BL/6J breeding pairs (8-10 weeks) were used to generate newborn mice, which were imaged at postnatal day 5. Mice were housed in a temperature-controlled room with a 12 hours light and 12 hours dark cycle and acclimated at least 3 days prior to animal experiments under specific pathogen-free conditions. All experiments were approved by the Institutional Animal Care and Use Committee (IACUC) of the Massachusetts General Hospital (MGH).

Myocardial infarction in mice

Coronary ligation was conducted under sterile conditions to induce MI in female or male mice (C57BL/6J) aged 8-12 weeks. Mouse thorax fur was removed and mice were anesthetized with 2% isoflurane. For disinfection, 80% isopropyl alcohol and betadine were applied on the surgical area, and mice were intubated with a 22G catheter for ventilation. The left fourth intercostal space was located, and a 0.5 cm incision was made. The epicardial tissue was carefully cut open. The left anterior descending artery was permanently ligated with an 8.0 nylon monofilament suture (Ethicon, Somerville, NJ). The intercostal space and the skin wound were closed with 5.0 nylon monofilament sutures (Ethicon, Somerville, NJ). Mice were extubated and allowed to recover on a heating pad. All mice received buprenorphine (0.1 mg/kg i.p.) twice for three days.

Cecal ligation and puncture in mice

Bacterial peritonitis was induced via cecal ligation and puncture (CLP) under sterile conditions. Mice were anesthetized with 2% isoflurane and anesthesia was maintained through nose cones. A 1 cm abdominal incision was made parallel to the linea alba. The linea alba was carefully cut

open to reveal the cecum. To induce mild-to-moderate peritonitis, ~0.6 cm of the cecal tip was ligated using a 5.0 nylon suture filament. A 22G needle was used to puncture the cecal wall, and a small amount of feces protruded into the peritoneal cavity. The linea alba was sutured using a 5.0 nylon monofilament. Mice received 0.5 mL saline for rehydration intraperitoneally. The skin was carefully stapled with 7 mm staples (Harvard Apparatus), and mice were allowed to recover on a heating pad. Buprenorphine was used for analgesia as described above.

Pneumonia in mice

Pneumonia was induced in mice with bioluminescent *streptococcus pneumoniae* Xen-10 strain A66.1 serotype 3 (Caliper, LifeSciences)¹. The bacterial colonies were cultured on Trypticase™ Soy Agar with 5% sheep blood (Fisher, BD Diagnostics) at 37°C and 5% CO₂ without aeration. Bacterial colonies were passaged daily onto new plates. To prepare for infection, bacterial colonies were transferred into Brain-Heart-Infusion broth (BHI, Sigma-Aldrich) containing 5% sheep blood (Carolina Biological Supply) and 200 µg/mL kanamycin (Sigma-Aldrich). Bacteria were allowed to grow for 3 hours. Bacterial concentration was estimated from optical density and bioluminescence. We chose a sublethal bacterial dose of ~1-2 x 10⁵ colony-forming units to infect 10-week-old female C57BL/6J mice. To this end, the mice's thorax fur was shaved. Mice were anesthetized with 2% isoflurane and intubated with a 22G catheter in an upright position. The corresponding volume of BHI broth was pipetted onto the catheter. After inhalation, mice were kept in an upright position to ensure full uptake of the bacterial dose. Bacterial bioluminescence was recorded with a combined bioluminescence/ X-ray scanner (AmiX, Spectral Instruments Imaging Co.) 24 and 48 hours after infection. The scanner was set at medium binning with exposure times between 20 seconds and 8 min. A corresponding X-ray was obtained after each bioluminescence scan to confirm anatomical localization of the signal. Bioluminescent images were analyzed with AMIView software (V2.8) and FIJI (NIH). Region of interests were placed over the lungs and background bioluminescence was subtracted. Signal strength was expressed as photons per second.

Rabbit model of atherosclerosis

Male New Zealand White (NZW) rabbits (2.5-3.0 months old) were purchased from Charles River Laboratories (Wilmington, MA). To induce the formation of atherosclerotic plaques, endothelial denudation of the aorta was performed. Anesthesia was induced in rabbits with an intramuscular (i.m.) administrations of ketamine (20 mg/kg) (Fort Dodge Animal Health, Overland Park, Kansas, USA) and xylazine (5 mg/kg) (Bayer AG, Leverkusen, Germany). The right femoral artery was identified and used to give access to a 4F-Fogarty embolectomy catheter (Edwards Lifesciences, Irvine, CA) which was inflated at the level of the left subclavian artery and slowly deflated while retracting until the iliac bifurcation, all performed under X-ray guidance (Philips Allura Xper FD20/10, Philips Healthcare, Amsterdam, The Netherlands). After 4 weeks, the procedure was repeated on the contralateral side. Two weeks before the first surgery mice began a cholesterol-rich diet of regular chow enriched with 0.3% cholesterol and 4.7% coconut oil (Research Diets, Inc. Brunswick, NJ), for a total of 8 weeks. Hereafter the diet was changed to a 0.15% enriched cholesterol diet that continued for the remaining months until experiments took place. Untreated healthy rabbits were fed a regular chow diet to serve as controls.

Coronary ligation surgery in rabbits

To induce myocardial infarction in rabbits, we permanently ligated the marginal artery branching from the left circumflex artery. Anesthesia was induced in rabbits with an intramuscular (i.m.) administrations of ketamine (20 mg/kg) (Fort Dodge Animal Health, Overland Park, Kansas, USA) and xylazine (5 mg/kg) (Bayer AG, Leverkusen, Germany). Rabbits were subsequently intubated for the remainder of the procedure and provided with a mixture of oxygen and isoflurane. During the surgical procedure, rabbits were additionally monitored using an ECG and pulse oximeter. After shaving the thorax, disinfection was performed using Povidone-iodine. A partial sternotomy was performed, after which the heart was visualized using a retractor. The

pericardium was opened using sharp curved Metzenbaum scissors. Using a Prolene 6-0, a permanent ligation was placed at the apex of the heart for maneuvering and to prevent any collateral artery formation. After identification of the first major branch from the left circumflex artery, a permanent ligation was placed using a Prolene 6-0. To confirm infarct development, purple coloring of the myocardium was observed while the ECG simultaneously displayed ST elevations. If there was no coloration, another marginal artery was identified and ligated. After the permanent ligation was placed, the pericardium was left open to prevent a possible tamponade. The sternum was closed using a Prolene 0-0, while muscles were approximated and the skin was closed². All rabbits were monitored and kept on oxygen until anesthesia wore off and independent breathing was observed. All animal experiments were performed in accordance with protocols approved by the Institutional Animal Care and Use Committees of Mount Sinai and followed National Institutes of Health guidelines for animal welfare.

Myocardial ischemia/reperfusion injury in mini-swine

Three male and three female Yucatan mini-swine (9 months old, average weight 45.4 kg) were purchased from Exemplar Genetics (Sioux Center, IA). Animals were allowed to acclimate for one week before PET/MR imaging. A bolus of amiodarone (1–3 mg/kg) was given intravenously. Atropine (0.1 mg/kg), amiodarone (3 mg/kg) and potassium acetate (20 mEq) in saline were continuously infused at the rate of 300 mL/hour for the duration of the procedure. A 7-Fr hockey-stick catheter (Cordis, Miami, FL) was advanced to the left coronary artery. After the coronary angiogram, a 0.014-inch guide wire (Abbott, Park, IL) was advanced into the LAD and a 8-mm-long, 4.0-mm NC TREC over-the-wire balloon (Abbott) was advanced to the proximal part of the coronary artery. The balloon was then inflated to 3–4 atm for 90 minutes followed by reperfusion. After confirmation of hemodynamic stability, animals were allowed to recover. Intramuscular injections of nitroglycerine and furosemide were administered. Intravenous saline with amiodarone, atropine and potassium acetate infusion was decreased to 50 mL/hour and given overnight. The animals were housed in their cages and monitored daily.

Flow cytometry

Mice received VT⁶⁸⁰Macrin intravenously 24 hours before sacrifice. A body weight-adjusted dose was administered to mice. Adult mice received 10 nmol VT680XL in 740 µg Macrin while 5-day-old mice received 2 nmol VT680XL in 128 µg Macrin. Under anesthesia with 2% isoflurane, the right heart auricle was cut off, and mice were perfused with 3-20 mL of phosphate buffered saline (adjusted to body weight) via cardiac puncture using a 22G needle. Hearts, lungs and aortas were carefully excised, and organ weights were recorded using a fine scale. Harvested organs were thoroughly minced in a digestion cocktail containing 450 U/mL collagenase I (Sigma), 125 U/mL collagenase XI (Sigma), 60 U/mL hyaluronidase I-S (Sigma), 60 U/mL DNase I (Sigma) and 20 µL/mL HEPES buffer (Mediatech Inc.) in PBS (Lonza). Samples were incubated on a shaker at 750 rpm for 1 hour at 37 °C. PBS containing 0.5% bovine serum albumin (FACS buffer) was used to filter tissue suspensions through 40 µm cell strainers. Samples were centrifuged at 340 g and 4°C for 7 min. The supernatants were discarded, and the cell pellets were diluted in 300 µL of FACS buffer. Cells were labeled with a lineage antibody mix and a selection of antibodies against myeloid and macrophage epitopes. The following antibodies were used: PE CD45R/B220 anti-mouse/human (Clone RA3-6B2, Biolegend); PE TER-119 rat anti-mouse (Clone TER-119, BD Pharmingen); PE CD49b anti-mouse (Clone DX5, Biolegend); PE CD90.2 anti-mouse (Clone 53-2.1;30-H12, Biolegend) and PE NK1.1 anti-mouse (Clone PK136, Biolegend); FITC-CD11b rat anti-mouse (Clone M1/70, Biolegend); PerCP/Cy5.5 rat anti-mouse Ly6C (Clone HK1.4, Biolegend); PE/Cy7 anti-mouse F4/80 (Clone BM8, Biolegend); BV421 CD64 anti-mouse (Clone X54-5/7.1, Biolegend); PE Ly6G rat anti-mouse (Clone 1A8, BD Pharmingen); FITC, PE/Cy7 CD11b anti-mouse/human (Clone M1/70, Biolegend); BV510 anti-mouse CD11c (Clone N418, Biolegend); PerCP/Cy5.5 CD31 anti-mouse (Clone 390, Biolegend); BV421 rat anti-mouse Siglec-F (Clone E50-2440 BD Biosciences); BV605 anti-mouse I-A/I-E (Clone M5/144.15.2, Biolegend); BV711 rat anti-mouse

CD45 (Clone 30-F11, BD Bioscience); APC/Cy7 Ly6G anti-mouse (Clone 1A8, Biolegend); APC/Cy7 CD3 anti mouse (Clone 17A2, Biolegend); APC/Cy7 CD19 anti-mouse (Clone 6D5, Biolegend); PE MEFSK4 anti-mouse (Clone mEF-SK4, Miltenyi Biotech); PE MHCII anti-mouse (Clone M5/114.15.2, Biolegend); BV605 CCR2 anti-mouse (Clone SA203G11, Biolegend). All samples were incubated in a 1:100-1:600 dilution at 4°C for 30 min. Next, samples were washed in 1 mL FACS buffer and centrifuged as described above. Data were recorded using a LSR2 flow cytometer. FlowJo X 10.0 software (Treestar) was used for analysis. A hematocytometer was used to obtain cell numbers per sample. Cardiac macrophages were identified as lineage^{low} Ly6G^{low} CD11b^{high} CD64^{high} F4/80^{high} Ly6C^{low} or CD45^{high} Ly6G^{neg} CD11b^{high} CD64^{high}. Cardiac and aortic fibroblasts were identified as CD45^{neg} CD31^{neg} MEFSK4^{pos} and endothelial cells as CD45^{neg} CD31^{high}. Alveolar macrophages were identified as CD11c^{high} SSC-A^{high} MHCII^{low} CD64^{high} Siglec-F^{high} CD11b^{low}. Lung interstitial macrophages were identified as CD11c^{intermediate} SSC-A^{low} MHCII^{high} CD64^{high} CD11b^{high} Siglec-F^{low}. Aortic lymphocytes were identified as CD45^{high} CD11b^{neg} lineage^{pos}, aortic neutrophils as CD45^{high} CD11b^{pos} lineage^{pos}, aortic macrophages as CD45^{high} CD11b^{pos} lineage^{neg} Ly6C^{low} F4/80^{pos}, and aortic monocytes as CD45^{high} CD11b^{pos} lineage^{neg} Ly6C^{high} F4/80^{low}.

Ex vivo biodistribution in mice

After PET/CT imaging, mice were euthanized and perfused with PBS (2-20 mL) through the left ventricle prior to organ harvesting. Excised organs were weighed, and radioactivity of organs was measured using a gamma counter (1480 Wizard 3-inch, PerkinElmer, Waltham, MA). Percent injected dose per gram tissue was calculated after corrections of radioisotope decay and residual activity at the injection site.

Biodistribution of ⁶⁴Cu-macrin in healthy mice for human dosimetry

The whole organ distribution of ⁶⁴Cu-Macrin was evaluated in healthy adult mice (C57BL/6J, 9 weeks old, 23.2 ± 3.0 g, mean ± S.D.) at 1 h, 4 h, 24 h and 48 h post-injection (4 females and 4 males per time point). Mice received tail-vein injections of ⁶⁴Cu-Macrin (0.040 ± 0.007 µg/g, 6.6 ± 1.1 µCi/g in 130 ± 10 µL) under anesthesia (2% isoflurane with 1 L/min O₂). Mice were euthanized and perfused with PBS (20 mL) through the left ventricle prior to organ harvesting. The following tissues and organs were collected: brain, blood, lungs, liver, spleen, right kidney, empty bladder, left rectus femoris muscle, fat, heart, brain, left femur bone, adrenals, empty stomach, empty small intestine, urine, uterus, ovaries and testes. Excised organs were weighed and subjected to radioactivity measurement using a gamma counter (1480 Wizard 3-inch, PerkinElmer, Waltham, MA). Biodistribution data were obtained after corrections for radioisotope decay and residual activity at the injection site.

Triphenyltetrazolium staining and autoradiography of mouse heart tissue

To visualize the infarct area, sliced myocardium (1 mm) was incubated with freshly prepared 1% triphenyltetrazolium chloride (TTC, Sigma Aldrich) in PBS for 30 min at 37 °C. Stained tissues were fixed in 10% formalin for 20 min and then captured with a digital flatbed scanner (HP Scanjet). Tissue uptake and distribution of ⁶⁴Cu-Macrin in myocardium was imaged by digital autoradiography. The tissue was placed on a film cassette and exposed on a storage phosphor screen (GE Healthcare) for 10 hours at room temperature. The phosphor screen was scanned at a pixel resolution of 25 µm with a Typhoon 9410 (Amersham Bioscience). The data were processed using ImageQuant software (Amersham Biosciences) or FIJI (NIH).

Cellular uptake of ⁶⁴Cu-Macrin in myocardium

Mice (C57BL/6, 8-12-wk) received ⁶⁴Cu-Macrin (190.6±11.9 µCi) intravenously via tail vein. Hearts were harvested 24 hours post injection. Macrin heart tissue uptake was measured by a scintillation counting. Cells were isolated using the same method that was performed for flow cytometric analysis in this manuscript, which yields a cell suspension and excludes matrix and the extracellular spaces. In brief, heart tissue was digested with enzyme cocktail for 1 hour at 37 °C after mincing the tissues into small pieces. The homogenized mixtures were passed through cell strainers (40 µm), washed and centrifuged to yield a cell pellet. The supernatant containing ECM was carefully removed without disturbing the cell pellet. After dehydration for 35 min at 95 °C, the dried cells were weighed. Radioactivity was measured using a gamma counter (1480 Wizard 3-inch, PerkinElmer, Waltham, MA). Macrin cell accumulation was calculated after corrections for radioisotope decay and residual activity at the injection site.

Ex vivo confocal microscopy

Ischemic heart injury and peritonitis were induced in Cx3cr1^{GFP/+} mice on a C57BL/6 background (5-day-old and 8-10-week old animals) as described in the surgery section. Mice received rhodamine-labeled lectin (Vector Labs, CA) via retro-orbital injection (20-200 µg) 30 min prior to imaging. Organs were harvested 24 hours post i.v. injection of ^{VT680}Macrin (10 nmol VT680XL in 740 µg Macrin for adult mice via tail vein injection and 2 mol VT680XL in 148 µg Macrin for 5-day-old mice via retroorbital injection) after perfusion with PBS (2-20 mL). Excised tissues were placed on glass slides with a few drops of PSB and covered with cover slips. Images were acquired using a FluoView FV1000MPE confocal imaging system (Olympus America). 473, 559 and 635 nm lasers were used with dichroic beam filters (DM473/559/635 nm), beam splitters (SDM473, SDM560, and SDM 640) and emission filters (BA490-540, BA575-620, and BA575-675) (all Olympus America). Confocal images were analyzed using FIJI (NIH). To quantify GFP expressing macrophages in Cx3cr1^{GFP/+} mice, Z-projection of 3D images were created. Confocal images with the same tissue thickness and the same magnification were analyzed. After background subtraction and thresholding, fluorescent areas were quantified, and percent GFP+ area was calculated from the total area.

Histology

After in vivo imaging, organs were excised from mice, pigs and rabbits and fixed in 10% formalin solution. Paraffin-embedded tissue sections were deparaffinized and rehydrated prior to staining. H&E staining (Vector Laboratories) was performed to identify cell and tissue morphology. Before IHC for tissue macrophages, heat-induced epitope retrieval (HIER) methods (Retrievagen A pH 6.0, BD Biosciences) and proteolytic-induced epitope retrieval (PIER) methods (Proteinase K, DAKO/Agilent) were performed for mouse and pig macrophage staining and rabbit macrophage staining, respectively.

Mouse aortic roots and hearts were fixed in 4% paraformaldehyde in PBS overnight. After rinsing in PBS, roots and hearts were placed in 30% sucrose in PBS overnight and embedded in OCT compound. Serial sections were prepared and stained with CD68 (clone: FA-11, BioLegend) for macrophages, CD31(clone: MEC13.3, BD Biosciences) for endothelial cells, alpha smooth muscle Actin (ab5694, Abcam) and Periostin (ab14041, Abcam) for fibroblasts, and Wheat Germ Agglutinin Oregon Green 488 Conjugate (Invitrogen) for cardiomyocytes. Goat anti-Rat IgG Alexa Fluor 488 and Goat anti-Rabbit IgG Alexa Fluore 488 (Invitrogen) were applied and DAPI was used for nuclear counterstaining. Images were acquired using BX63 (Olympus) and processed with Fiji ImageJ software.

For IHC, endogenous peroxidase activity was quenched by 1% hydrogen peroxide. To prevent nonspecific antibody binding, tissues were incubated with 4% normal horse serum or 4% normal rabbit serum. After rinsing, tissues were treated with primary antibodies for macrophages: a pig macrophage antibody (Clone: BA4D5, Bio-Rad Laboratories), a rabbit macrophage antibody (Clone: RAM11, Dako/Agilent) or a mouse Mac-3 antibody (Clone: M3/84, BD Biosciences),

accordingly. After overnight incubation at 4 C° and rinsing, secondary antibodies (biotinylated horse anti-mouse IgG/biotinylate rabbit anti rat IgG, Vector Laboratories) were applied to detect macrophages using an Avidin-Biotin Complex Kit (VECTASTAIN Elite ABC HRP Kit, Vector Laboratories). AEC (3-amino-9-ethylcarbazole) substrate-chromogen (DAKO/Agilent) was used as a peroxidase substrate to form a red end-product on the target antigen in macrophages, and the sections were counterstained with Harris Hematoxylin (Sigma-Aldrich). *Streptococcus pneumoniae* in lung tissues were visualized using a Gram Staining Kit (MilliporeSigma). Slides were scanned by a digital slide scanner (NanoZoomer 2.0RS, Hamamatsu), and images were analyzed with NDP.view2 and FIJI (NIH).

Human dosimetry estimation

Internal human radiation dose was estimated by Organ Level Internal Dose Assessment (OLINDA/EXM, v.1.0) using biodistribution data from mice (Table S1)³. Animal data was extrapolated to obtain human dosimetry using the direct and the mass extrapolation methods in (ref⁴). To account for the blood inside each organ, we have used standard values of blood volume on the main organs (i.e. brain, kidney, liver, lungs, small intestine, spleen and testes) as described⁵. For other organs without a specific blood volume, blood was assumed proportionally distributed on the organ based on the relative mass of the organ with respect to the whole-body. Blood volume (mL) per organ was converted to mass (mg) using the density of mouse blood as described⁶. Blood doses per organ were assigned proportionally to the amount of blood mass per organ and added to the calculated organ doses. The cumulative activity (Bq-h/Bq) for each source organ was determined by integrating the area under the time-activity curves using the least-squares analysis. The absorbed dose to the bladder was calculated using the OLINDA bladder model assuming voiding after 1.5 hours, and the dose to the organs was calculated assuming homogeneous distribution of the activity throughout the organ. We conservatively assumed that the pharmacokinetics of urinary clearance was identical to the bi-exponential whole-body clearance, and fractions (0.29 and 0.2 for females and 0.21 and 0.22 for males) and biological half-times (0.03 h and 3.44 h for females and 0.03 h and 2.43 h for males) were used in the voiding bladder model of OLINDA/EXM. Effective doses were calculated in accordance with ICRP-60 organ weighting factor recommendations⁴.

Toxicity testing of Macrin in rodents

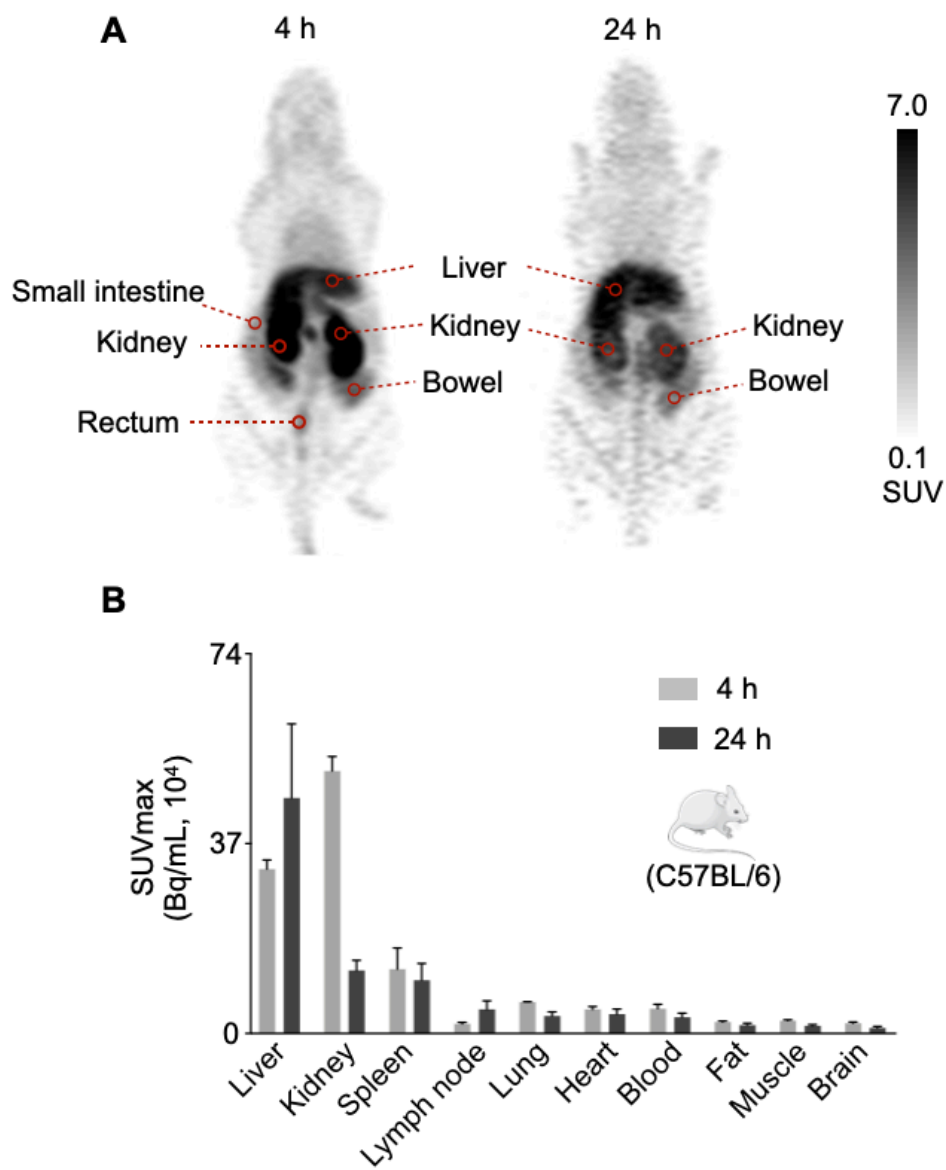
Sixty Sprague-Dawley rats were used to obtain data on nanoparticle toxicity (Sai Life Sciences Ltd). A single dose of Macrin-NODA solution at 0.13 and 1.3 mg/kg was injected intravenously, which is 100 and 1,000 times higher than the anticipated human dose (5-7 weeks old, female and male, n=5 per sex and group). Macrin-NODA was intravenously administered at doses of 0.13 mg/kg and 1.3 mg/kg. Control group rats received vehicle only and were handled in a similar manner as the treatment group. Mortality and morbidity were checked at least twice a day during the study period. Clinical signs were recorded at least once a day throughout the study period. Observations included, but were not limited to, evaluation of changes at injection site; changes in skin and fur, eyes and mucous membranes; respiratory, circulatory, autonomic, and central nervous systems; somatomotor activity and behavior patterns. Body weights were recorded periodically during the study period. Rats were subjected to blood sample collection from retro-orbital plexus under light isoflurane anesthesia for clinical pathology analyses. All the animals fasted for 16-18h before blood collection. Following blood collections for clinical pathology 24 hours and 14 days after Macrin administration, rats were euthanized by carbon dioxide asphyxiation. All rats were subjected to a detailed gross pathological examination that included careful examination of the external surface of the body, all orifices and the cranial, thoracic and abdominal cavities and their contents. Major organs, including heart, spleen, thymus, lungs, kidneys and adrenals were processed using standard methods and embedded in paraffin for histopathology. Tissue sections were stained with hematoxylin-eosin and examined by a pathologist.

Gamma counting and autoradiography in large animals

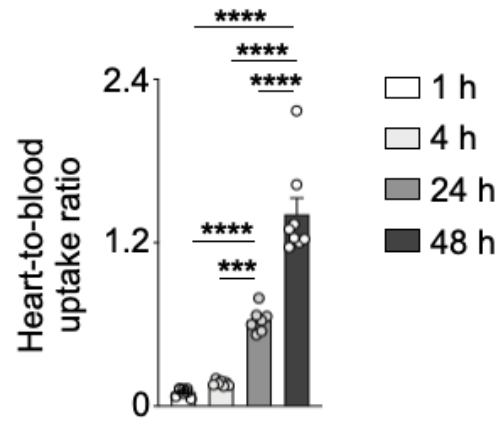
⁶⁴Cu-Macrin uptake in tissues and blood was measured by gamma counting. Shortly after the scan, animals were euthanized. Rabbits and pigs were thoroughly perfused with saline before tissues of interest (liver, spleen, kidney, lung, muscle, bone marrow, bone and heart) were harvested. Rabbit aortas were carefully dissected and rinsed with saline. Samples were weighed and radioactivity was measured on a Wizard2 2480 automatic gamma counter (Perkin Elmer). Radioactivity values were corrected for decay and normalized to tissue weight to express radioactivity concentration as percentage injected dose per gram or kilogram (%ID/g or %ID/kg). Digital autoradiography was performed to determine ⁶⁴Cu-Macrin distribution within the heart. Hearts were sliced from the apex to the atria. Samples were placed in a film cassette against a phosphorimaging plate (BASMS-2325, Fujifilm, Valhalla, NY) for 41 hours (rabbit aortas) or 39 hours (rabbit heart slices) at -20 °C. Phosphorimaging plates were read at a pixel resolution of 25 µm with a Typhoon 7000IP plate reader (GE Healthcare, Pittsburgh, PA).

Online References

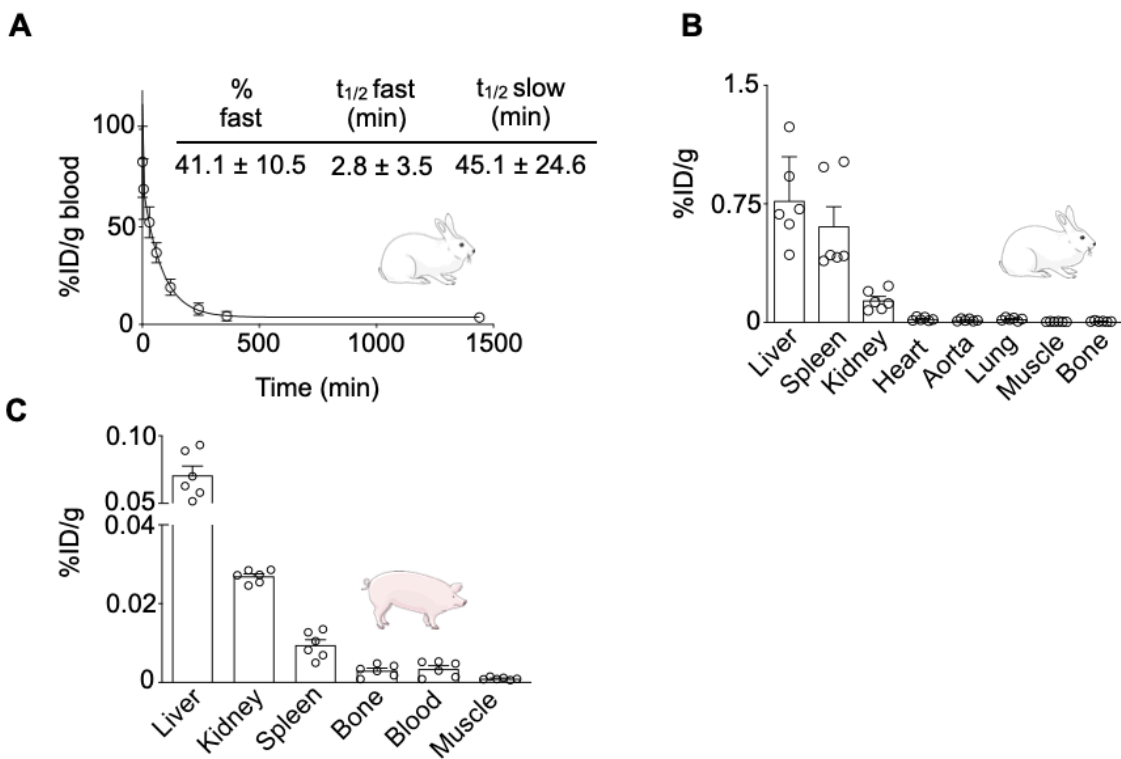
1. Davis RW, Eggleston H, Johnson F, Nahrendorf M, Bock PE, Peterson T, Panizzi P. In Vivo Tracking of Streptococcal Infections of Subcutaneous Origin in a Murine Model. *Molecular Imaging and Biology*. 2015;17:793-801.
2. Tan MY, Xia B, Xiao Z, Fan ZW, Zhou H, Guo X, Huang YC. Development of a new model for acute myocardial infarction in rabbits. *J Vet Med Sci*. 2017;79:467-473.
3. Stabin MG, Sparks RB, Crowe E. OLINDA/EXM: the second-generation personal computer software for internal dose assessment in nuclear medicine. *The Journal of Nuclear Medicine*. 2005;46:1023.
4. 1990 Recommendations of the International Commission on Radiological Protection. *Ann ICRP*. 1991;21:1-201.
5. Kaliss N, Pressman D. Plasma and blood volumes of mouse organs, as determined with radioactive iodoproteins. *Proc Soc Exp Biol Med*. 1950;75:16-20.
6. Riches AC, Sharp JG, Thomas DB, Smith SV. Blood volume determination in the mouse. *J Physiol*. 1973;228:279-284.



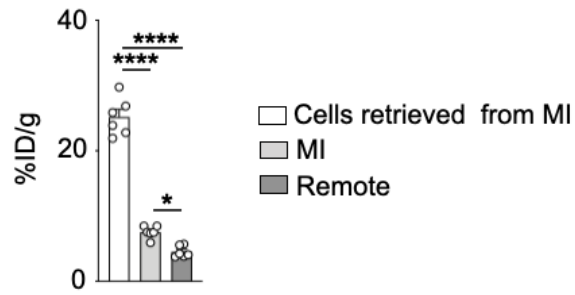
Online Fig. I. Biodistribution of ⁶⁴Cu-Macrin in C57BL/6 mice. (A) Coronal PET images at 4 h and 24 h post injection. **(B)** SUV reflecting ⁶⁴Cu-Macrin uptake at 4 h (n=2 mice) and 24 h (n=5) post injection. LN, lymph node. Data are mean ± SD.



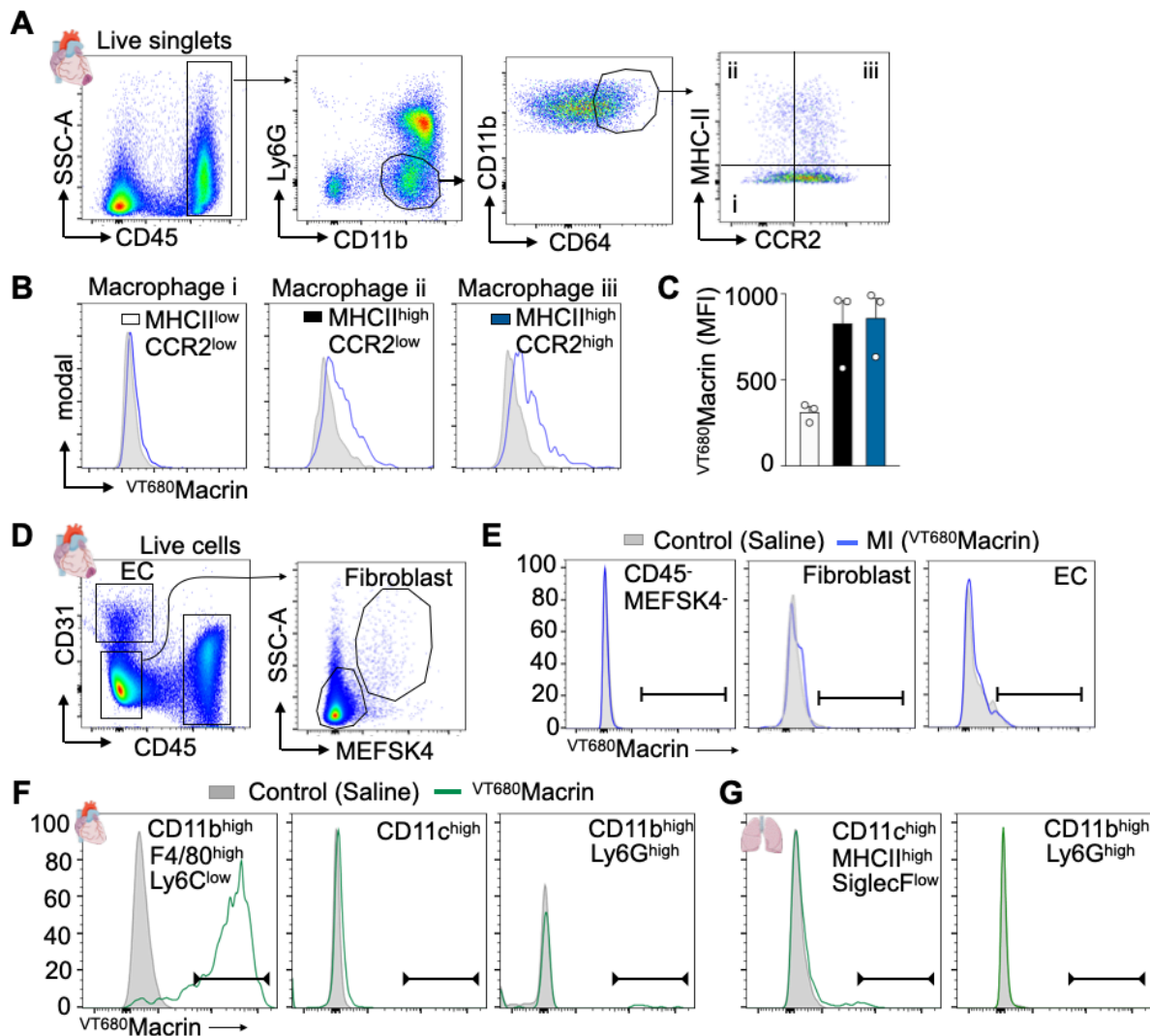
Online Fig. II. ^{64}Cu -Macrin heart-to-blood signal ratio. Heart to blood uptake ratio in healthy mice at 1, 4, 24 and 48 h post ^{64}Cu -Macrin injection (n=8, mean \pm SEM).



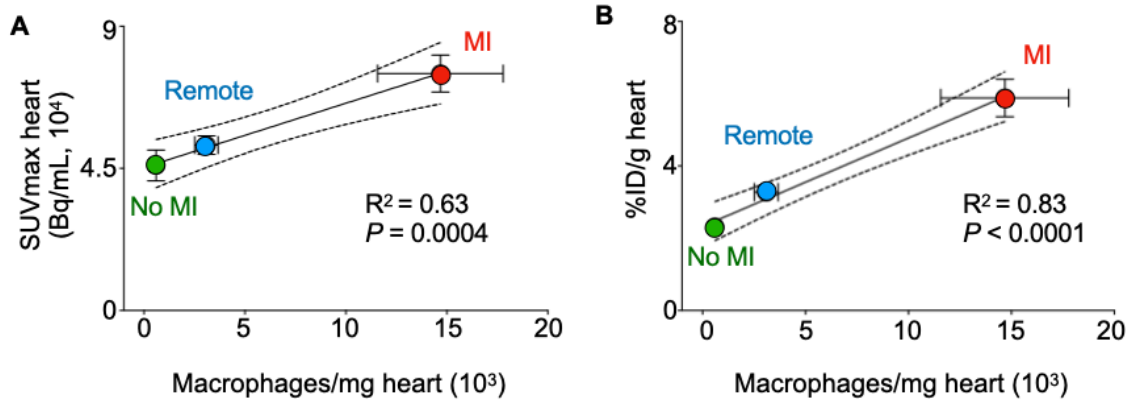
Online Fig. III. Pharmacokinetics and biodistribution of ^{64}Cu -Macrin in rabbits and pigs. (A) Blood half-life of ^{64}Cu -Macrin in healthy rabbits ($n=6$, mean \pm SEM). (B) Biodistribution of ^{64}Cu -Macrin in rabbits and (C) pigs 24 h post-injection (mean \pm SEM).



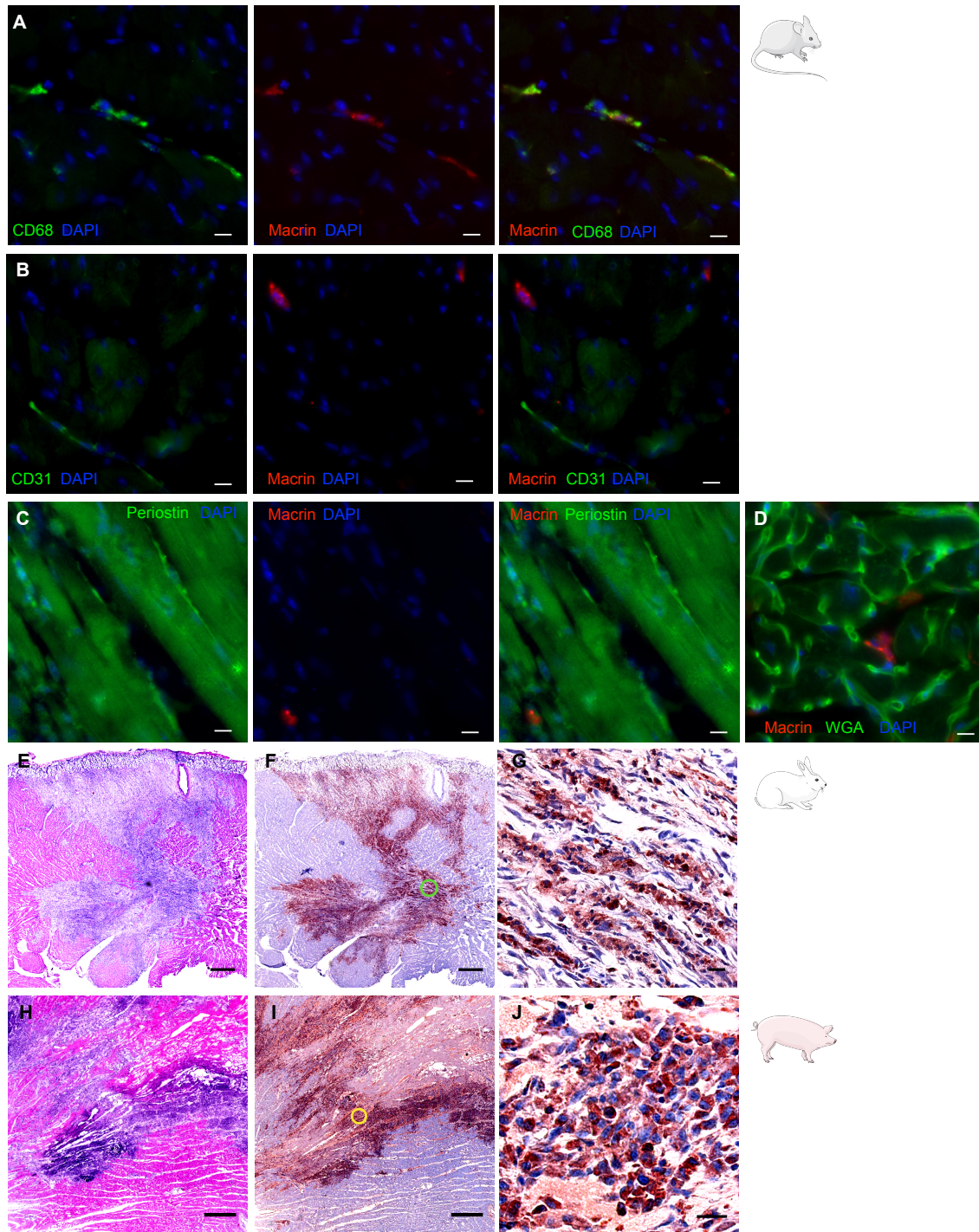
Online Fig. IV. ⁶⁴Cu-Macrin cellular accumulation. Cells from hearts on day 4 after MI and myocardium were subjected to scintillation counting 24 hours post injection of ⁶⁴Cu-Macrin (n=6 mice, mean±SEM).



Online Fig. V. VT_{680} Macrin accumulation in various cells assessed by FACS. (A) Flow cytometry gating and **(B)** histograms for VT_{680} Macrin fluorescent intensity for heart macrophage subsets (grey, saline injected control; blue VT_{680} Macrin injected mice with MI). **(C)** Mean fluorescence intensity (MFI) for cell subset, $n=3$ mice, mean \pm SEM. **(D)** Gating for heart fibroblasts and endothelial cells (EC). **(E)** No uptake was observed in heart fibroblasts and EC. **(F)** VT_{680} Macrin uptake in cardiac macrophages (left panel), $CD11c^+$ dendritic cells (middle) and neutrophils (right). **(G)** VT_{680} Macrin uptake in $CD11c^{\text{high}}$, $MHCII^{\text{high}}$, $Siglec^{\text{low}}$ cells in lung (left) and neutrophils (right).

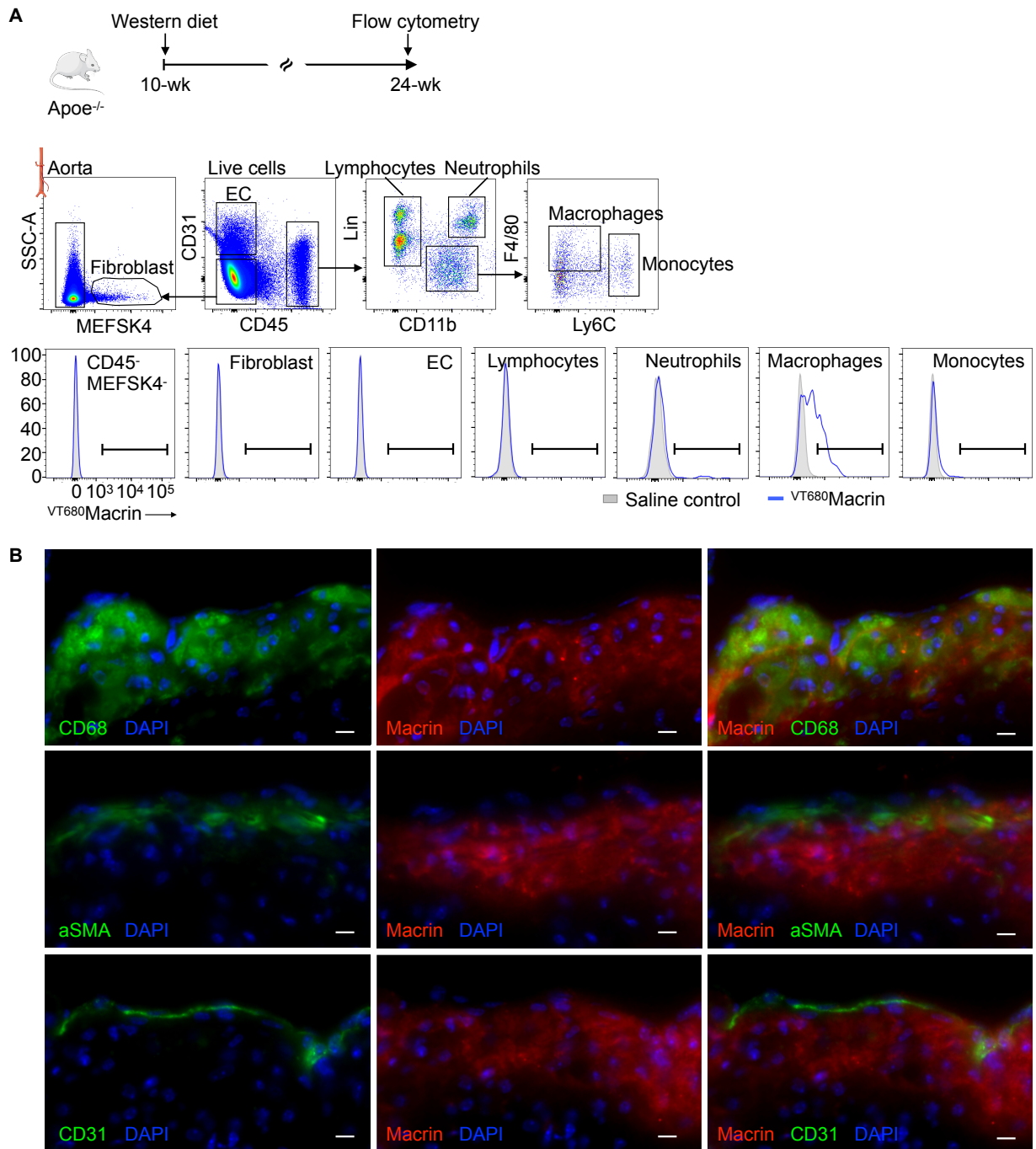


Online Fig. VI. Correlation of ^{64}Cu -Macrin tissue concentration with cardiac macrophage density. In vivo PET signal intensities were quantified in SUVmax. Ex vivo Macrin uptake was obtained by scintigraphy. Macrophage numbers were calculated from flow cytometry and correlated with ^{64}Cu -Macrin tissue signal measured in vivo (**A**) and ex vivo (**B**).



Online Fig. VII. Histology of infarct tissue in mice, rabbits and pigs. (A)

Immunofluorescence histology in a mouse heart 2 days after MI showing VT680 Macrin uptake into CD68⁺ macrophages but not into (B) endothelial cells, (C) fibroblasts or (D) cardiomyocytes (scale bar, 10 μ m). (E) H&E staining of rabbit heart day 3 post MI (scale bar, 0.5 mm). (F) Immunohistochemistry staining for macrophages in the same tissue. (G) High magnification of infarcted myocardium (scale bar, 20 μ m). (H) H&E staining of pig heart day 3 post MI (scale bar, 0.5 mm). (I) Immunohistochemistry staining for macrophages in the same tissue (scale bar, 0.5 mm). (J) High magnification of infarcted myocardium (scale bar, 20 μ m).



Online Fig. VIII. Macrin cellular distribution in atherosclerotic plaques. (A) Aortic cells were identified by FACS gating as indicated. Fluorescence intensity corresponding to ^{VT680}Macrin uptake is shown in histograms. Blue, ^{VT680}Macrin injected mice with atherosclerosis (representative plots of n=3 mice) compared to saline injected mice with atherosclerosis (grey). **(B)** Immunoreactive staining for CD68⁺ macrophages, aSMA⁺ fibroblasts, CD31⁺ endothelial cells and ^{VT680}Macrin fluorescence in aortic root plaques of ApoE^{-/-} mice with atherosclerosis (scale bar, 10 μm).

disease model	species	intervention	goal	number of animals
acute MI	mouse	coronary ligation	image increase of infarct macrophages	5 control 5 MI
acute MI	mouse	coronary ligation	define cellular uptake of Macrin in heart by FACS and histology	7 control 5 MI
acute MI	rabbit	coronary ligation	image increase of infarct macrophages in large animal	6 control 5 MI
acute MI	pig	90 min balloon occlusion	image increase of infarct macrophages in large animal	6 control 6 MI
newborn heart	mouse	none	image increase of resident macrophages	5 adult 9 newborn
newborn heart	mouse	none	FACS and histology validation in newborn	7 adult 6 newborn
heart in sepsis	mouse	induction of sepsis by cecal ligation and puncture	image increase in heart macrophages during sepsis	5 control 6 sepsis
heart in sepsis	mouse	induction of sepsis by cecal ligation and puncture	FACS and histology validation of heart in sepsis	7 control 4 sepsis
lung after MI	mouse	coronary ligation	image fluctuation of lung macrophages after MI	7 control 8 MI
lung after MI	mouse	coronary ligation	FACS and histology validation in lung after MI	4 control 5 MI
pneumonia	pig	none / accidental finding	image increase of lung macrophages in bacterial pneumonia	8
pneumonia	mouse	intratracheal bacterial instillation	image increase of lung macrophages in pneumonia	7 control 19 pneumonia
atherosclerosis	rabbit	balloon denudation atherogenic diet	image plaque macrophages	6 control 6 atherosclerosis
atherosclerosis	mouse	ApoE ^{-/-} mouse atherogenic diet	define cellular uptake of Macrin in plaques	5 atherosclerosis

Online Table I. Experimental overview, species and animal numbers. The table summarizes animal models and what they were used for in this study.

%ID/g	1 h	4 h	24 h	48 h
Liver	28.090 ± 2.610	35.420 ± 6.660	36.040 ± 11.400	32.210 ± 6.910
Kidney	22.470 ± 3.610	23.030 ± 5.920	15.170 ± 2.810	9.640 ± 0.890
Blood	19.840 ± 3.690	11.750 ± 2.090	4.176 ± 1.111	1.860 ± 0.530
Spleen	8.280 ± 2.230	10.600 ± 2.450	16.230 ± 4.950	12.170 ± 4.000
Uterus	5.520 ± 1.590	4.520 ± 1.280	4.720 ± 0.820	3.470 ± 1.150
Ovaries	4.880 ± 0.590	4.070 ± 0.850	5.843 ± 5.102	3.920 ± 1.280
Small intestine	4.650 ± 0.470	4.100 ± 0.720	4.300 ± 1.030	3.300 ± 0.620
Stomach	4.400 ± 0.980	4.460 ± 0.540	3.860 ± 1.030	2.850 ± 0.370
Bladder	4.640 ± 4.140	2.580 ± 1.020	2.370 ± 0.860	1.670 ± 0.610
Lung	2.900 ± 1.450	2.840 ± 1.530	3.630 ± 2.020	3.360 ± 1.370
Adrenal	2.600 ± 0.850	3.070 ± 0.640	4.650 ± 0.740	4.460 ± 2.110
Heart	2.000 ± 0.510	2.010 ± 0.320	2.640 ± 0.740	2.510 ± 0.470
Bone	1.770 ± 0.430	1.750 ± 0.410	2.780 ± 1.380	1.790 ± 0.450
Testis	1.330 ± 0.150	1.630 ± 0.230	1.940 ± 0.160	1.470 ± 0.100
Muscle	0.500 ± 0.170	0.400 ± 0.080	0.510 ± 0.130	0.450 ± 0.090
Fat	0.390 ± 0.110	0.310 ± 0.090	0.530 ± 0.290	0.420 ± 0.110
Brain	0.160 ± 0.060	0.140 ± 0.040	0.270 ± 0.060	0.280 ± 0.060

Online Table II. Ex vivo biodistribution of ⁶⁴Cu-Macrin in healthy mice (C57BL/6, n=4 per sex/time point). Organs were excised at 1, 4, 24 and 48 hours post injection and subjected for scintigraphy. Data are shown in mean ± SD.